Chemical Papers (2020) 74:2101–2109
https://doi.org/10.1007/s11696-020-01056-x

ORIGINAL PAPER

Biomimetic synthesis of magnesium oxide nanoparticles using *Chromolaena odorata* (L.) leaf extract

Enobong R. Essien[1] · Violette N. Atasie[1] · Taiye O. Oyebanji[1] · Davies O. Nwude[1]

Received: 13 September 2019 / Accepted: 8 January 2020 / Published online: 20 January 2020
© Institute of Chemistry, Slovak Academy of Sciences 2020

Abstract

The green method for preparing metal and metal oxide nanoparticles is increasingly becoming popular as a result of its eco-friendliness compared with physical and chemical methods. The biomolecules inherent in plant extracts are known to serve as reductants and capping agents to form metal/metal oxide nanoparticles. This study, therefore, aimed to synthesize magnesium oxide nanoparticles (MgONPs) using the aqueous extract of *Chromolaena odorata* leaf. The type of phytochemicals present in the leaf extract was initially examined in a gas chromatograph–mass spectrometer (GC–MS). UV–visible (UV–Vis) spectrophotometric assessment indicated the formation of MgONPs by developing a peak at 270 nm, scanning electron microscopy (SEM) showed good surface properties, energy-dispersive X-ray analysis (EDX) confirmed the presence of MgO in the sample, transmission electron microscopy (TEM) revealed cubic-shaped MgONPs with average size 12.3 nm, X-ray diffractometry (XRD) confirmed the formation of MgO phase and Fourier transform infrared (FTIR) spectroscopy supported the capping role of the phytochemicals identified by GC–MS. Thermo-gravimetric analysis (TGA) and differential thermal analysis (DTA) was further employed to study weight differentials during treatment and to corroborate the results of the GCMS and FTIR. The obtained MgONPs showed potential for application in catalysis and as antimicrobial agent. Since the plant used is a weed and is ubiquitous, the reported synthesis process could be upscaled for commercial production of MgONPS.

✉ Enobong R. Essien
reggiessien@gmail.com

[1] Department of Chemical and Food Sciences, Bells University of Technology, P.M.B 1015, Ota, Ogun, Nigeria

Graphic abstract

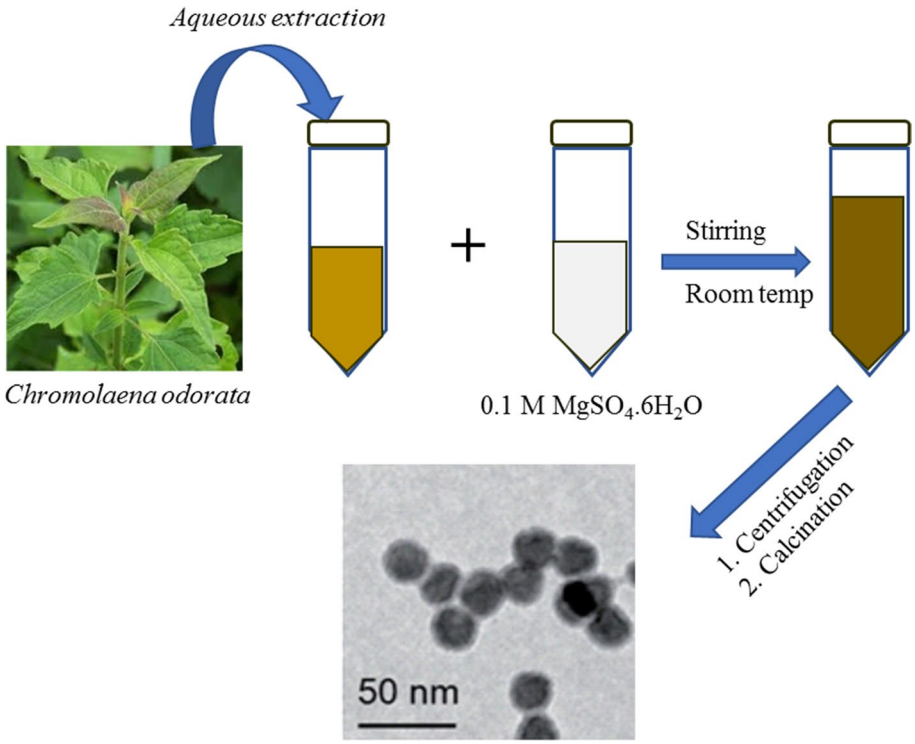

Keywords Magnesium nanoparticles · *Chromolaena odorata* · Aqueous leaf extract · Phytochemicals · Green synthesis · Capping agent

Introduction

Nanotechnology has produced materials of various types at the nanoscale level, which is 1–100 nm in dimension (Laurent et al. 2010). Since the past few decades, nanotechnology has recorded tremendous progress in the synthesis of nanoparticles, nanolayers, powders, optoelectronics, and mechanical nanodevices as well as nanostructured biological materials. Currently, several types of metal oxides nanoparticles have been applied in numerous areas of Physics, Chemistry, Materials science, and Biomedicine (Abdallah et al. 2012). Some metals can form a large miscellany of metal oxides with structural geometries having an electronic structure that can exhibit semiconductor, metallic or insulator properties. Metal oxide nanoparticles are used in optoelectronics, microelectronic circuits, sensors, fuel cells and piezoelectric devices among others.

Metal oxide nanoparticles exhibit unique chemical and physical properties as well as stability (Suresh et al. 2014) due to their high density and the limited size of their corner or edge. There are several types of metal oxide nanoparticles, such as ZnO, CuO, TiO_2, MgO, NiO, and ZrO_2. Unique among them is MgO nanoparticles (MgONPs), which possess antimicrobial properties, but non-toxic to humans. MgONPs have demonstrated antimicrobial ability against *E. coli* (Jin and He 2011; Zhang et al. 2012), *Staphylococcus aureus* (Bindhu et al. 2016), and have shown great potential in its antagonistic action against Xoo (Abdallah et al. 2019), the pathogen of rice bacterial blight. Further investigations reveal that MgONPs have interesting applications in medicine, such as relieving heartburn, initiating post-activation of bone repair when used as scaffolds and acting as hyperthermia agents in cancer therapy (Martinez-Boubeta et al. 2010). Furthermore, MgONPs are applied in biomolecular detection, diagnostics, and microelectronics (Shrivastava 2018).

The green synthesis technique of metal oxide nanoparticles has evolved over the years due to the benefit of using plant materials along with water as a benign solvent, thereby making the process moderately pollutant-free (Moorthy et al. 2015). Other advantages of the method include low energy consumption and mild reaction conditions (e.g. low temperature and pressure), absence of catalyst, and, importantly, the cost-effectiveness of the process (Mie et al. 2014). By contrast, chemical and physical techniques are expensive and, sometimes, hazardous to the environment as a result of the toxic and unsafe reagents used as well as the toxic

by-product released into the environment during the synthesis (Hazarika et al. 2014).

Metal oxide nanoparticle synthesis via the green approach has involved the use of many organisms such as yeast, molds, algae, bacteria, sugars, polymers (chitosan), and plant extracts. For plant-mediated synthesis, the inherent phytochemicals present in the plant extracts, including various water-soluble plant metabolites (e.g. alkaloids, phenolic compounds, and terpenoids) and co-enzymes (Bonomo 2018), act as reducing and capping agents to form the nanoparticles.

For nanoparticles synthesized from plant leaf extracts, the extracts are mixed with an appropriate metal precursor to form a solution. The rate of formation, morphology, and stability of the nanoparticles are determined by parameters such as types and concentration of phytochemicals in the plant extract, metal–salt concentration, pH and temperature of the reaction media (Dwivedi and Gopal 2010).

The reducing action is carried out on the metal oxide precursors by the phenolic compounds and compounds containing hydroxyl groups present in the plant extracts. Stabilization of nanoparticle growth is promoted by amino acids, protein, and lipids present in the plant extracts which can act as biological surfactants (Tripathy et al. 2010). According to the mechanism described by Tripathy et al. 2010, after the metal nanoparticles form in solution, they are stabilized to prevent van der Waals forces from causing coagulation. During the stabilization process, which may occur in several ways: steric or electrosteric barriers or purely electrostatic barriers may be created around the particle surface by physisorbed surfactants and polymers. In many cases, chemical adsorption, which involves direct covalent bonding with the surface metal atoms occurs. Physisorption via electrostatic interaction also takes place, but to a lesser extent, giving rise to either charge-induced dipole mechanisms or dispersion force mechanisms or both. The outcome is the formation of metal/metal oxide nanoparticles surrounded by bioorganic capping agents, which are also responsible for the stability of the nanoparticles.

In general, three steps are involved in the synthesis of metal/metal oxide nanoparticles from plant extracts (Si and Mandal 2007): (i) the activation phase—bioreduction of metal ions/salts and nucleation process of the reduced metal ions); (ii) the growth phase—spontaneous combination of tiny particles with greater ones, called Ostwald ripening; (iii) the termination phase—determines the final shape of the nanoparticles.

Chromolaena odorata (L.) is commonly known as Siam weed and is a fast-growing perennial and invasive weed. It is native to South and Central America and belongs to the family *Asteraceae*. It has several medicinal uses: anti-diarrheal, astringent, antispasmodic, anti-hypertensive, anti-inflammatory, and diuretic (Iwu et al. 1999). Extract from its flowers is used as tonic, antipyretic and heart tonic (Bunyapraphatsara and Chokechaijaroenporn 2000). Besides, the leaves are used by communities in the southern part of Nigeria for wound dressing, skin infection and to stop bleeding.

The medicinal properties of plants, generally, have been attributed to phytochemicals, such as alkaloids, tannins, flavonoids and other phenolic compounds, which produce a definite physiological action on the human body (Vaghasiya et al. 2011). Interestingly, the edibility of *Chromolaena odorata* is not well documented, thus making it attractive as widely available plant material for possible large-scale preparation of MgONPs, without any potential significant adverse effect on the ecological food chain. Therefore, our aim in this study is to synthesize MgONPs using *Chromolaena odorata* leaf extract, which to the best of our knowledge is yet to be reported in the literature.

Experimental

Materials

The *Chromolaena odorata* leaves used for this experiment were collected from the premises of the Bells University of Technology, Ota, Ogun State, Southwest, Nigeria, and validated at the Botany Department of University of Lagos, Nigeria. The reagent chemicals: $MgSO_4{\cdot}6H_2O$ and absolute ethanol were purchased from Sigma-Aldrich.

Preparation of *Chromolaena odorata* aqueous leaf extract

The leaves of *Chromolaena odorata* were initially washed with tap water and then rinsed with deionized water to remove dust and particulate impurities. Thereafter, they were dried under sunlight and pulverized into fine powder to impart a large surface to increase the rate of solvent absorption. The powdered sample (48 g) was mixed with 250 mL of deionized water, sealed and boiled for 15 min in a thermostatic water bath. The mixture was allowed to cool to room temperature, then filtered to obtain the aqueous extract and eventually stored in a refrigerator between 5 and 10 °C for further use.

Synthesis of MgONPs

To prepare the MgONPs, *Chromolaena odorata* aqueous leaf extract (250 mL) was added in drops to 0.1 M solution of $MgSO_4{\cdot}6H_2O$ (50 mL) in a conical flask under a constant stirring condition with a magnetic stirrer, the addition procedure consumed a total time of 12 h. The pH of the medium at the end of the reaction was 3.6. The resulting solid–liquid dispersion was centrifuged at 7000 rpm for

15 min. Afterward, the supernatant was discarded while the residue was washed with deionized water to get rid of excess $MgSO_4{\cdot}6H_2O$ and residual organic compounds. The residue was dried in an oven at 70 °C for 2 h and then calcined at 500 °C for 3 h using NETZSCH STA 409 CD at a heating rate of 5 °C/min to perform thermogravimetric analysis (TGA) and differential thermal analysis (DTA) of the obtained MgONPs to study the decomposition profile of the sample. To obtain dispersed MgONPs, the sample was sonicated in ethanol at 40 °C for 1 h in an ultrasonic cleaner. The process is summarized in the flowchart depicted in Fig. 1.

The *Chromolaena odorata* aqueous leaf extract was analyzed in a gas chromatograph–mass spectrometer (GC–MS) (Shimadzu QP2010SE) (with specification: VWD: 257 nm; temperature: ambient; flow rate: 0.5 mL/min; column: SMT OD-5-100/15, C18 150 × 4.6 mm, injection ratio: EtOH:HOH 1:1) using helium gas to identify the phytochemicals responsible for the possible reduction reaction and stabilization to form the MgONPs. Thereafter, the fragmentation patterns obtained were used to identify the phytochemicals present in the extract. UV–Vis absorption spectrophotometer (Uniscope SM 7504) was used to monitor the formation of MgONPs by measuring the wavelength of absorption between 100 and 700 nm during the reaction between $MgSO_4{\cdot}6H_2O$ and the *Chromolaena odorata* leaf extract.

Assessment of the microstructure to evaluate particle distribution and elemental composition of the MgONPs was performed in a scanning electron microscope (SEM) equipped with an energy-dispersive X-ray analyzer (EDX) unit (SEM: JEOL JSM 7660F). The sample was attached to a sample holder using a carbon adhesive, followed by gold sputtering before it was subjected to visual observation at an accelerating voltage of 15 kV.

To analyze for particle size and structure of the synthesized MgONPs, a single drop of the MgONPs (in an aqueous form) was carefully placed on a copper-coated grid and imaged on a transmission electron microscope (TEM) (TEM: JEM-ARM200F-G) using a 200-kV accelerating voltage. Then the average particle size was determined from the TEM micrograph using ImageJ software.

The diffraction pattern of the sample was obtained in an X-ray diffractometer (XRD) (XRD: Rigaku D/Max-IIIC) to assess the type of phases present and to assess the crystalline structure of the MgONPs.

To determine the type of bonds present in the MgONPs to complement and confirm the results of the GC–MS, UV, and XRD, Fourier transform infrared (FTIR) spectroscopy (FTIR: Nicolet iS10) with wavenumber in the range of 350–4000 cm^{-1} was employed.

Results and discussion

UV–Vis spectrophotometry

The size, shape, interaction between the particles, and the absorbed molecules present on the surface of the nanoparticles have a strong influence on the optical properties of metal nanoparticles. A sharp absorption band at 270 nm is observed in the UV–Vis absorption spectrum of the MgONP solution (Fig. 2) corresponding to the dipole resonance of MgO nanospheres, which is usually in the range 260–280 nm (Vergheese and Vishal 2018; Moorthy et al. 2015). This result implies that the biomolecules present in *Chromolaena odorata* leaf extract successfully reduced the $MgSO_4{\cdot}6H_2O$ to MgONPs. There were 24 phytochemicals identified in the extract, as shown in Table 1, but the ones in high

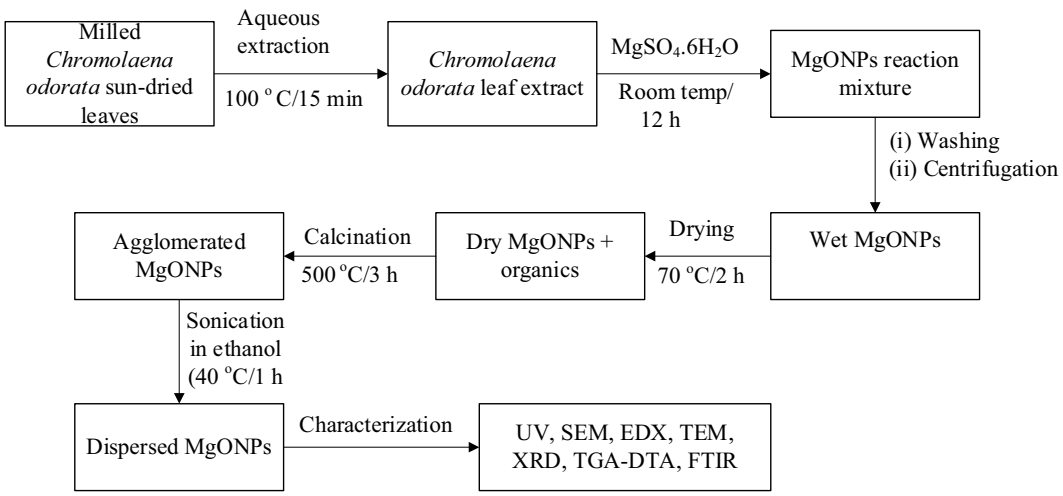

Fig. 1 Flowchart showing the preparation stages of the MgONPs

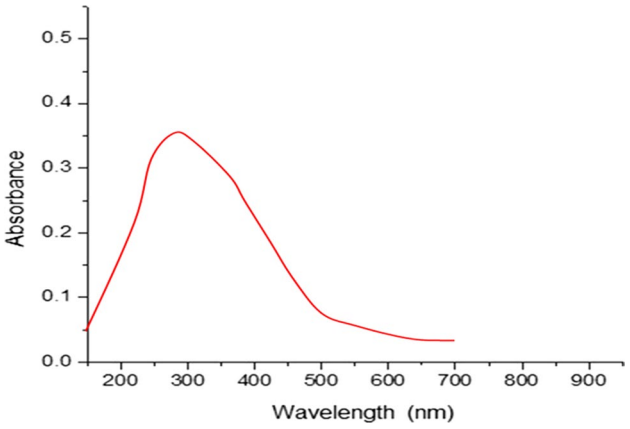

Fig. 2 UV–Vis spectrum of the colloidal solution of *Chromolaena odorata* leaf extract and $MgSO_4 \cdot 6H_2O$ showing maximum absorption at 270 nm due to the presence of MgONPs

concentration and, therefore, proposed for the bio-reduction reaction included glycerin, β-sitosterol, 7-oxabicyclo[4.1.0] heptan-2-ol, 1,6-dideoxydulcitol, I-heptadec-1-ynyl-cyclopentanol, 1-heptatriacotanol, 17-(1,5-dimethylhexyl)-2-hydroxyl-10,13-d, 1-naphthalenepropanol, Kauran-18-al and 2H-3,9a-methano-1-benzoxepin. All these biomolecules contain the functional groups –C–O–C, –C–O–, –C=C–, –C≡C–, and –C= O known to act as reducing agents in plant-based synthesis (Huang et al. 2007).

Morphological properties and elemental composition of the MgONPs

Figure 3 depicts the morphology of the MgONPs. The particles as shown in the microstructure appear heterogeneous in size and shape and are in different aggregates distributed over the surface of the material to present a large surface area. The type of surface morphology presented has been found to be useful in applications such as in catalysis

Table 1 GC–MS result showing all the phytochemicals identified in the *Chromolaena odorata* aqueous leaf extract along with their corresponding peak area

Peak	Retention time	Peak area (%)	Name of compound	Mol. weight	Mol. formula
1	7.564	1.55	Glycerin	92.094	$C_3H_8O_3$
2	9.587	0.53	Trans-1,4-cyclohexanediol	116.158	$C_6H_{12}O_2$
3	10.357	0.34	Benzoic acid, ethyl ester	150.17	$C_9H_{10}O_2$
4	11.099	0.90	2,2,3,3-Tetraethyloxirane	156.269	$C_{10}H_{20}O$
5	12.131	10.89	7-Oxabicyclo[4.1.0]heptan-2-ol	114.144	$C_6H_{10}O_2$
6	12.294	4.09	1,6-Dideoxydulcitol	150.174	$C_6H_{14}O_4$
7	13.745	0.95	1,4,2,5-Cyclohexanetetrol	148.16	$C_6H_{12}O_2$
8	15.313	1.83	1-Methyl-6-(3-methylbuta-1,3-dienyl)-7-oxabicyclo[4.1.0]heptane	178.27	$C_{12}H_{18}O$
9	15.550	2.50	Stevioside	804.88	$C_{38}H_{60}O_{18}$
10	15.735	1.63	1,7,7-Trimethylbicyclo[2.2.1]heptane-2,5-diol	170.252	$C_{10}H_{18}O_2$
11	15.941	1.37	*cis*-Z-alpha-bisabolene epoxide	220.356	$C_{15}H_{24}O$
12	16.153	1.14	*cis*-Z-alpha-bisabolene epoxide	220.356	$C_{15}H_{24}O$
13	16.920	1.23	1-Heptadec-1-ynyl-cyclopentanol	320.361	$C_{22}H_{40}O$
14	17.086	3.27	1-Heptatriacotanol	357	$C_{37}H_{76}O$
15	18.051	15.91	Beta-sitosterol	414.718	$C_{29}H_{50}O$
16	18.120	13.37	Beta-sitosterol	414.718	$C_{29}H_{50}O$
17	18.201	8.69	Beta-sitosterol	414.718	$C_{29}H_{50}O$
18	19.012	4.92	Methanesulphonic acid	96.1	CH_4O_3S
19	19.324	7.80	[(6R)-6-[(8R,9S,10S,13R,14S,17R)-10,13-Dimethyl-2,3,4,5,6,7,8,9,11,12,14,15,16,17-tetradecahydro-1H-cyclopenta[a] phenanthren-17-yl]-2-methylhepta-1,3-dienyl] benzoate	488.74	$C_{34}H_{48}O_2$
20	19.529	2.79	(1-(Naphthalen-1-yl)propan-1-ol	186.104	$C_{13}H_{14}O$
21	19.625	7.33	Kauran-18-al, 17-(acetyloxy-, (4.beta.)-	346.511	$C_{22}H_{34}O_3$
22	20.024	3.39	1-Naphthalenepropanol, alpha-ethenyldecahydro-3-hydroxy-alpha,5,5,8a-tetramethyl-2-methylene-	306.4828	$C_{20}H_{34}O_2$
23	20.274	2.86	2H-3,9a-Methano-1-benzoxepin, octahydro-2,2,5a,9-tetramethyl-, [3R-(3α,5aα,9α,9aα)]-	222.366	$C_{15}H_{26}O$
24	20.906	0.71	2H-3,9a-Methano-1-benzoxepin, octahydro-2,2,5a,9-tetramethyl-, [3R-(3α,5aα,9α,9aα)]-	222.366	$C_{15}H_{26}O$
		100			

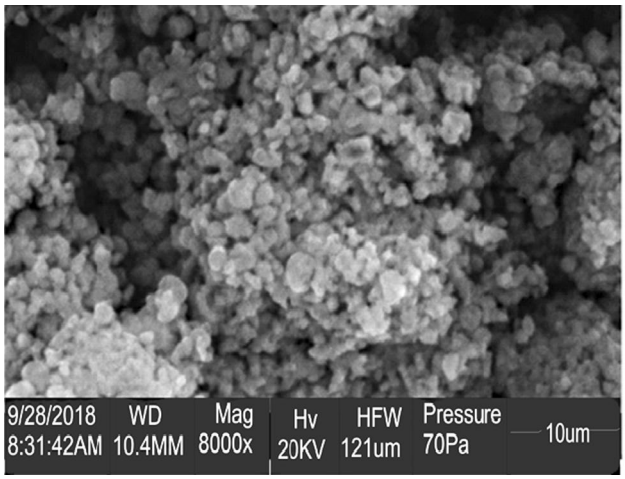

Fig. 3 SEM micrograph of the MgONPs showing well-distributed particles to present a large surface area

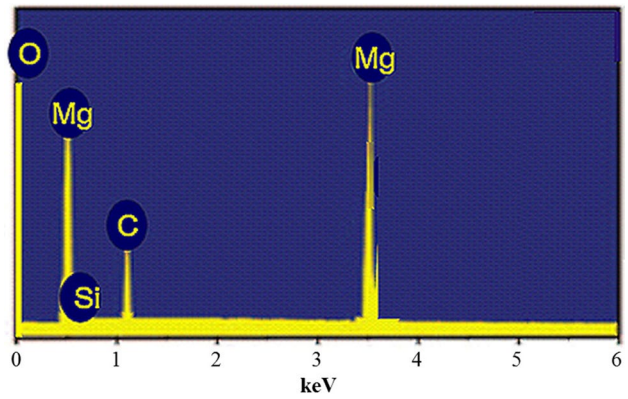

Fig. 4 EDX spectrum of the MgONPs showing the presence of Mg and O at 1:1 atomic ratio and C atom due to the presence of organic molecules

(Navalón and García, 2016) and biomedicine (Huang et al. 2007). Generally, in heterogeneous catalysis, metal oxide nanoparticles with large surface area function as the metal (Astruc 2008), thus resulting in a reaction rate of the order of magnitude far higher than those of the corresponding bulk materials.

The result of the elemental composition of the MgONPs investigated by EDX was further used to confirm the formation of MgO. As shown in the EDX spectrum (Fig. 4), Mg and O in the sample are present at high intensity and at the atomic ratio of 1:1 as found in pure MgO compound. The carbon atom seen in the spectrum is due to the residual organic biomolecules present in the sample from the plant extract which served as reducing and capping agents to produce the MgONPs.

Particle shape and size characteristics

The evaluation of the MgONPs to determine the particle size and structure was performed using TEM. As presented in Fig. 5, the particles were almost cubic in shape with an average size of 12. 3 nm. Figure 5a, b agrees with the SEM micrograph (Fig. 3) which showed well-distributed particles with some degree of aggregation. The heterogeneous nature of the particles, which was earlier observed in the SEM micrograph (Fig. 3) is more prominent in the TEM image presented in Fig. 5b. To a large extent, the ultrasonic radiation passed through the sample in ethanol medium in addition to the capping ability of the phytochemicals present in the plant extract (Kaur et al. 2017) was instrumental to the reduced degree of agglomeration and good dispersion of the particles. Efficient dispersion of particles is an important parameter that affects their interaction with the test media and is important in applications such as cytotoxicity (Kaur et al. 2017) and supported heterogeneous catalysis (Sharma et al. 2015; Navalón and García 2016).

Diffraction pattern of the MgONPs

The phase composition, crystalline structure and purity of the sample, as examined by XRD is depicted in the diffractogram in Fig. 6. The diffraction pattern shows peaks at

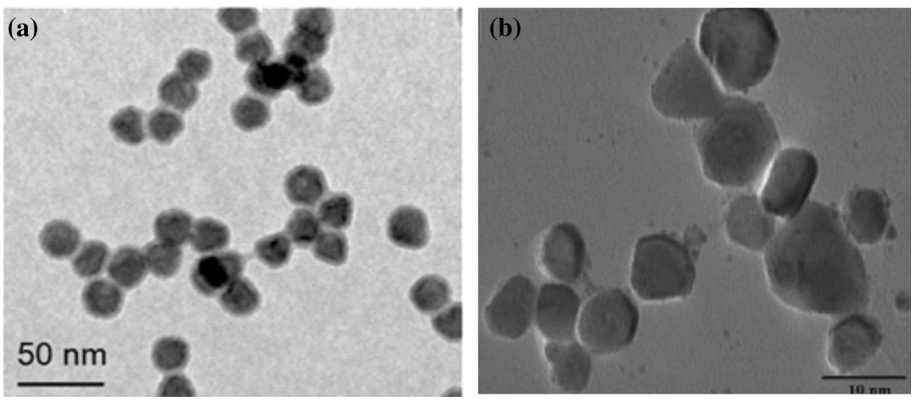

Fig. 5 The TEM image of the MgONPs showing monodisperse particles

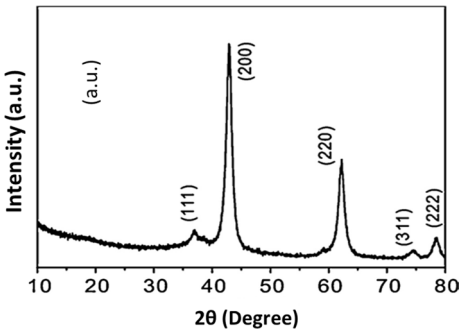

Fig. 6 XRD pattern of the MgONPs showing the formation of single-phase MgO

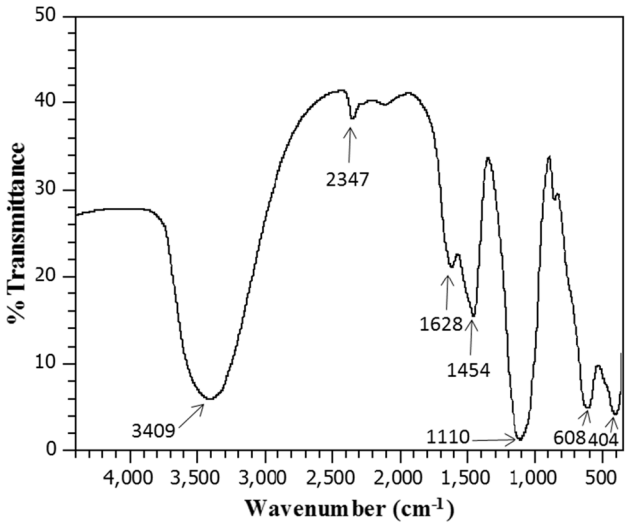

Fig. 7 FTIR spectrum of the synthesized MgONPs showing bonds related to the capping biomolecule contained in the *M. esculenta* leaf extract and MgO

hkl (111), (200), (220), (311) and (222) reflection planes. Examination of the peaks at both angular location and intensity shows that they match those in the standard reference file (JCDPS no. 75-0447), which confirms the formation of MgO phase (Safaei-Ghomia 2015), as indicated earlier in the EDX result (Fig. 4). There are no other peaks observed in the spectrum, which suggests the absence of metallic impurities and further supports the EDX result (Fig. 4).

Bond properties of the MgONPs

The FTIR spectrum of the MgONPs is shown in Fig. 7 shows that the broad band centred at 3409 cm^{-1} is due to the stretching vibration of O–H group in alcohol (Dobrucka 2016) and surface water (Moorthy et al. 2015). The OH group is supported by the prominent peak at 1454 cm^{-1} attributed to the bending mode of OH bond. The OH group could have emanated from the hydroxyl groups of the phytochemicals in the leaf extract involved in the capping reaction to form the MgONPs. The presence of water in the sample is further confirmed by the shoulder around 1628 cm^{-1} (Moorthy et al. 2015). The peak located at 2347 cm^{-1} is considered for C≡C bond stretching vibrations in alkyne, which is diffusive suggesting that the alkyne is present in low concentration in the sample. The presence of alkyne, in particular, confirms the GC–MS result which indicated the presence of the compound 1-heptadec-1-ynyl-cyclopentanol in the extract.

The peak located at 1110 cm^{-1} is associated with C–O diagnostic bonds (Somanathan et al. 2016), while the peaks around 608 and 404 cm^{-1} are assigned to stretching vibration of Mg–O bond (Vergheese and Vishal 2018).

Thermal analysis

The TGA–DTA curves showing the weight loss profile of the sample during the calcination process is presented in Fig. 8. There are two major weight-loss regimes, from 39 to 400 °C in the TGA. The weight losses between the temperatures of 70 °C and 118 °C corresponding to a 3.33% and 19.17%, respectively, are the result of dehydration occurring in the sample caused by the further loss of water molecules after the initial drying at 70 °C. During the second regime between 322 and 400 °C, a more significant weight loss of 31.43% is observed. This is due to the thermal decomposition of some of the organic moiety in the phytochemicals serving as capping agent and reductant, especially the decarboxylation of carboxyl groups to carbon (iv) oxide gas (Doreswamy et al. 2005). This, therefore, explains why carbonyl peak was absent in the FTIR spectrum shown in Fig. 7, even though it was detected in the plant extract phytochemicals as observed in the result of the GC–MS (Table 1).

The DTA curve shows two peaks. The strong endothermic peak at 118 °C corresponds to the removal of physically adsorbed as well as chemically bound water (Amarghan and Amini 2017). The exothermic peak at 421 °C is associated with the burning out of carbonaceous materials in the sample.

Conclusions

The green approach has been adopted to synthesize MgO nanoparticles using the aqueous extract from *Chromolaena odorata* leaf. Several organic biomolecules identified in the leaf extract by GC–MS were considered to act as synergistically as reductant and capping agents for forming the MgO nanoparticles. The formation of MgO nanoparticles was confirmed by UV–Vis spectrophotometry, SEM/EDX, TEM, XRD, and FTIR analysis. The MgONPs possessed an

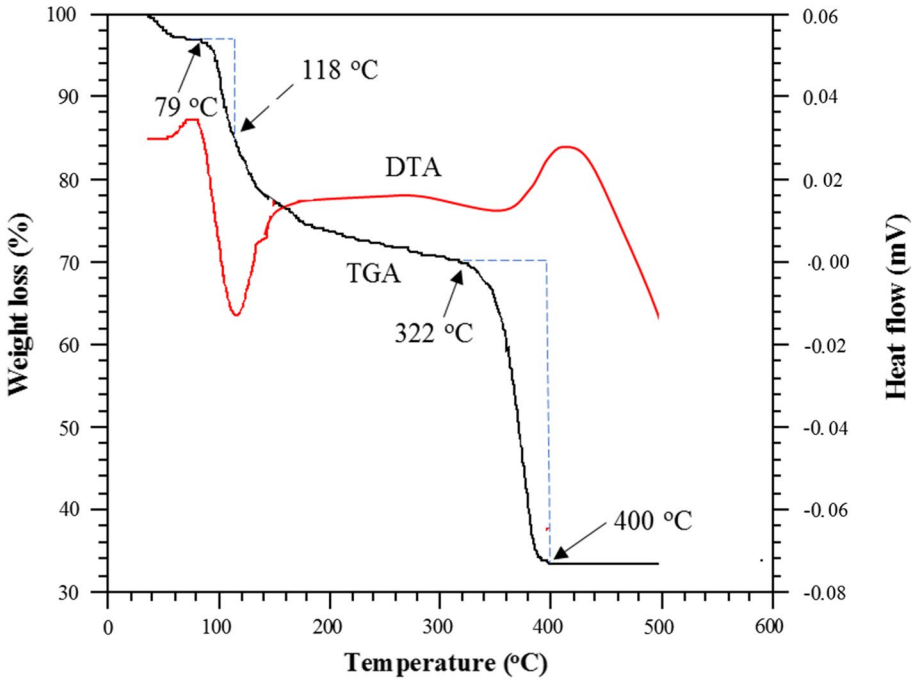

Fig. 8 TGA–DTA showing the thermal profile of the calcined MgONPs

average particle diameter of 12.3 nm, well dispersed with large surface area for potential application in biomedicine and catalysis. A significant achievement of this study is the use of *Chromolaena odorata*, a weed that forms a large percentage of the vegetation in the tropical region of the world. This implies that an envisaged large-scale production of MgONPs using *Chromolaena odorata* could be sustainable. Besides, the approach established in this study would make it is possible to obtain well-dispersed, high-purity MgO nanoparticles with a large surface area.

Acknowledgements The authors are grateful to the Department of Food and Chemical Sciences, Bells University of Technology, Ota, for providing equipment and material support for this study.

Compliance with ethical standards

Conflict of interest On behalf of all authors, the corresponding author states that there is no conflict of interest.

References

Abdallah Y, Ogunyemi O, Abdelazez A, Zhang M, Hong X, Ibrahim E, Hossain A, Fouad H, Andreescu S, Ornatska M, Erlichman JS, Estevez A, Leiter JC (2012) Biomedical applications of metal oxide nanoparticles. In: Matijević E (ed) Fine particles in medicine and pharmacy. Springer, Boston, pp 57–100

Abdallah Y, Ogunyemi O, Abdelazez A, Zhang M, Hong X, Ibrahim E, Hossain A, Fouad H, Li B, Chen J (2019) The green synthesis of MgO nano-flowers using *Rosmarinus officinalis* L. (Rosemary) and the antibacterial activities against *Xanthomonas oryzae* pv. *Oryzae*. BioMed Res Int. Article ID 5620989. https://doi.org/10.1155/2019/5620989

Armaghan M, Amini MM (2017) Adsorption of diazinon and fenitrothion on nanocrystalline magnesium oxides. Arab J Chem 10:91–99. https://doi.org/10.1016/j.arabjc.2014.01.002

Astruc D (2008) Nanoparticles and catalysis. Wiley, New York

Bindhu MR, Umadevi M, Micheal MK, Arasu MV, Al-Dhabi NA (2016) Structural, morphological and optical properties of MgO nanoparticles for antibacterial applications. Mater Lett 166:19–22. https://doi.org/10.1016/j.matlet.2015.12.020

Bonomo M (2018) Synthesis and characterization of NiO nanostructures: a review. J Nanopart Res 20:222. https://doi.org/10.1007/s11051-018-4327-y

Bunyapraphatsara N, Chokechaijaroenporn O (2000) Thai medicinal plants. Fac Pharm Mahidol Univ Natl Center Genet Eng Biotechnol Bangkok 4:622–626

Dobrucka R (2016) Synthesis of MgO nanoparticles using *Artemisia abrotanum* herbal extract and their antioxidant and photocatalytic properties. Iran J Sci Technol Trans Sci 42:547–555. https://doi.org/10.1007/s40995-016-0076-x

Doreswamy B, Mahendra M, Sridhar M, Shashidhara Prasad J, Varughese P, George J, Varghese G (2005) A novel three-dimensional polymeric structure of crystalline neodymium malonate hydrate. Mater Lett 59:1206–1213. https://doi.org/10.1016/j.matlet.2004.12.029

Dwivedi AD, Gopal K (2010) Biosynthesis of silver and gold nanoparticles using *Chenopodium album* leaf extract. Colloids Surf A Physicochem Eng Asp 369:27–33. https://doi.org/10.1016/j.colsurfa.2010.07.020

Hazarika D, Phukan A, Saikia E, Chetia B (2014) Phytochemical screening and synthesis of silver nanoparticles using leaf extract of *Rhynchotechum ellipticum*. Int J Pharm Pharm Sci 6:672–674

Huang J, Chen C, He N, Hong J, Lu Y, Qingbiao L, Shao W, Sun D, Wang XH, Wang Y, Yiang X (2007) Biosynthesis of silver and gold nanoparticles by novel sundried Cinnamomum camphora leaf. Nanotechnol 18:105–106. https://doi.org/10.1088/0957-4484/18/10/105104

Iwu MM, Duncan AR, Okunji CO (1999) New antimicrobials of plant origin. In: Janick J (ed) Perspectives on new crops and new uses. ASHS Press, Alexandria, pp 457–462

Jin T, He Y (2011) Antibacterial activities of magnesium oxide (MgO) nanoparticles against foodborne pathogens. J Nanopart 13:6877–6885. https://doi.org/10.1007/s11051-011-0595-5

Kaur I, Ellis L-J, Romer I, Tantra R, Carriere M, Allard S, Mayne-L'Hermite M, Minelli C, Unger W, Potthoff A, Rades S, Valsami-Jones E (2017) Dispersion of nanomaterials in aqueous media: towards protocol optimization. J Vis Exp 130:56074. https://doi.org/10.3791/56074

Laurent S, Forge D, Port M, Roch A, Robic C, Vander Elst L, Muller RN (2010) Magnetic iron oxide nanoparticles: synthesis, stabilization, vectorization, physicochemical characterizations, and biological applications. Chem Rev 110:2574–2574. https://doi.org/10.1021/cr900197g

Li B, Chen J (2019) The green synthesis of MgO nano-flowers using *Rosmarinus officinalis* L. (Rosemary) and the antibacterial activities against *Xanthomonas oryzaepv. oryzae*. BioMed Res Int. https://doi.org/10.1155/2019/5620989

Martinez-Boubeta C, Balcells L, Cristofol R, Sanfeliu C, Rodriguez E (2010) Self-assembled multifunctional Fe/MgO nanospheres for magnetic resonance imaging and hyperthermia. Nanomed Nanotechnol Biol Med 6:362–370. https://doi.org/10.1016/j.nano.2009.09.003

Moorthy SK, Asho CH, Rao KV, Viswanathana C (2015) Synthesis and characterization of MgO nanoparticles by neem leaves through green method. Mater Today Proc 2:4360–4368. https://doi.org/10.1016/j.matpr.2015.10.027

Mie R, Samsudin MW, Din LB, Ahmad A, Ibrahim N, Adnan SNA (2014) Synthesis of silver nanoparticles with antibacterial activity using the lichen Parmotrema praesorediosum. Int J Nanomed 9:121–127. https://doi.org/10.2147/IJN.S52306

Navalón S, García H (2016) Nanoparticles for catalysis. Nanomater (Basel) 6:123. https://doi.org/10.3390/nano6070123

Safaei-Ghomia J, Zahedia S, Javida M, Ghasemzadeh MA (2015) MgO nanoparticles: an efficient, green and reusable catalyst for the one-pot syntheses of 2,6-dicyanoanilines and 1,3-diarylpropyl malononitriles under different conditions. J Nanostruct 5:153–160. https://doi.org/10.7508/jns.2015.02.010

Sharma N, Ojha H, Bharadwaj A, Pathak DP, Sharma RK (2015) Preparation and catalytic applications of nanomaterials: a review. RSC Adv 5:53381–53403. https://doi.org/10.1039/C5RA06778B

Shrivastava S (2018) Synthesis of MgO nanoparticle by Neem leaves obtained from local area of Kotni village, Chhattisgarh through green method. Eur J Biomed Pharm Sci 5:746–747. https://www.ejbps.com

Si S, Mandal TK (2007) Tryptophan-based peptides to synthesize gold and silver nanoparticles: a mechanistic and kinetic study. Chem A Eur J 13:3160–3168. https://doi.org/10.1002/chem.200601492

Somanathan T, Krishna VM, Saravanan V, Kumar R, Kumar R (2016) MgO nanoparticles for effective uptake and release of doxorubicin drug: pH sensitive controlled drug release. J Nanosci Nanotechnol 16:9421–9431. https://doi.org/10.1166/jnn.2016.12164

Suresh J, Yuvakkumar R, Nathanael AJ, Sundrarajan M, Hong SI (2014) Antibacterial and wash durability properties of untreated and treated cotton fabric using MgO and NiO nanoparticles. Appl Mech Mater 508:48–51

Tripathy A, Raichur AM, Chandrasekaran N, Prathna TC, Mukherjee A (2010) Process variables in biomimetic synthesis of silver nanoparticles by aqueous extract of *Azadirachta indica* (Neem) leaves. J Nanopart Res 12:237–246. https://doi.org/10.1007/s11051-009-9602-5

Vergheese M, Vishal SK (2018) Green synthesis of magnesium oxide nanoparticles using Trigonella foenum-graecum leaf extract and its antibacterial activity. J Pharmacogn Phytochem 7:1193–1200

Vaghasiya Y, Dave R, Chanda S (2011) Phytochemical analysis of some medicinal plants from western region of India. Res J Med Plants 5:567–576. https://doi.org/10.3923/rjmp.2011.567.576

Yiang X (2007) Biosynthesis of silver and gold nanoparticles by novel sundried *Cinnamomum camphora* leaf. Nanotechnol 18:105–106. https://doi.org/10.1088/0957-4484/18/10/105104

Zhang K, An Y, Zhang L, Dong Q (2012) Preparation of controlled nano-MgO and investigation of its bactericidal properties. Chemosphere 89:1414–1418. https://doi.org/10.1016/j.chemosphere.2012.06.007

Publisher's Note Springer Nature remains neutral with regard to jurisdictional claims in published maps and institutional affiliations.